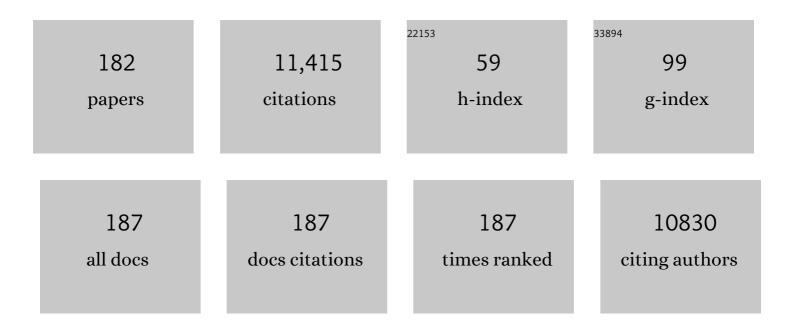
Michael J Therien

List of Publications by Year in descending order

Source: https://exaly.com/author-pdf/9515497/publications.pdf Version: 2024-02-01



#	Article	IF	CITATIONS
1	Biochemistry and Theory of Proton-Coupled Electron Transfer. Chemical Reviews, 2014, 114, 3381-3465.	47.7	399
2	Pushâ^'Pull Arylethynyl Porphyrins:  New Chromophores That Exhibit Large Molecular First-Order Hyperpolarizabilities. Journal of the American Chemical Society, 1996, 118, 1497-1503.	13.7	355
3	Near-infrared-emissive polymersomes: Self-assembled soft matter for in vivo optical imaging. Proceedings of the National Academy of Sciences of the United States of America, 2005, 102, 2922-2927.	7.1	355
4	Facile elaboration of porphyrins via metal-mediated cross-coupling. Journal of Organic Chemistry, 1993, 58, 5983-5993.	3.2	257
5	Controlled fabrication of nanogaps in ambient environment for molecular electronics. Applied Physics Letters, 2005, 86, 043109.	3.3	257

6 Bioresorbable Vesicles Formed through Spontaneous Self-Assembly of Amphiphilic Poly(ethylene) Tj ETQq0 0 0 rgBT /Overlock 10 Tf 50

7	Acetylenyl-Linked, Porphyrin-Bridged, Donorâ^Acceptor Molecules:  A Theoretical Analysis of the Molecular First Hyperpolarizability in Highly Conjugated Pushâ^'Pull Chromophore Structures. Journal of the American Chemical Society, 1996, 118, 1504-1510.	13.7	238
8	The Role of Porphyrinâ€ŧoâ€Porphyrin Linkage Topology in the Extensive Modulation of the Absorptive and Emissive Properties of a Series of Ethynyl―and Butadiynylâ€Bridged Bis―and Tris(porphinato)zinc Chromophores. Chemistry - A European Journal, 1995, 1, 645-651.	3.3	223
9	Design, Synthesis, Linear, and Nonlinear Optical Properties of Conjugated (Porphinato)zinc(II)-Based Donorâ^'Acceptor Chromophores Featuring Nitrothiophenyl and Nitrooligothiophenyl Electron-Accepting Moieties. Journal of the American Chemical Society, 2005, 127, 9710-9720.	13.7	192
10	Polymersomes: A new multi-functional tool for cancer diagnosis and therapy. Methods, 2008, 46, 25-32.	3.8	191
11	Ultrafast Dynamics of Highly Conjugated Porphyrin Arrays. Journal of the American Chemical Society, 1998, 120, 11489-11498.	13.7	186
12	Suzuki Porphyrins:  New Synthons for the Fabrication of Porphyrin-Containing Supramolecular Assemblies. Journal of the American Chemical Society, 1998, 120, 12676-12677.	13.7	173
13	Computational De Novo Design and Characterization of a Four-Helix Bundle Protein that Selectively Binds a Nonbiological Cofactor. Journal of the American Chemical Society, 2005, 127, 1346-1347.	13.7	167
14	Exceptional Near-Infrared Fluorescence Quantum Yields and Excited-State Absorptivity of Highly Conjugated Porphyrin Arrays. Journal of the American Chemical Society, 2006, 128, 9000-9001.	13.7	165
15	Spectroscopy, Electronic Structure, and Electrochemistry of [5,15-Bis[(aryl)ethynyl]- 10,20-diphenylporphinato]zinc(II) Complexes. X-ray Crystal Structures of [5,15-Bis[(4â€-fluorophenyl)ethynyl]- 10,20-diphenylporphinato]zinc(II) and 5.15-Bis[(4â€-methoxyphenyl)ethynyl]-10.20-diphenylporphyrin, lournal of the American Chemical Society.	13.7	163
16	1996, 118, 11854-11864. Helical Wrapping of Single-Walled Carbon Nanotubes by Water Soluble Poly(<i>p</i> -phenyleneethynylene). Nano Letters, 2009, 9, 1414-1418.	9.1	162
17	Additive engineering for high-performance room-temperature-processed perovskite absorbers with micron-size grains and microsecond-range carrier lifetimes. Energy and Environmental Science, 2017, 10, 2365-2371.	30.8	157
18	Unusual Frequency Dispersion Effects of the Nonlinear Optical Response in Highly Conjugated (Polypyridyl)metalâ^'(Porphinato)zinc(II) Chromophores. Journal of the American Chemical Society, 2002, 124, 13806-13813.	13.7	155

#	Article	IF	CITATIONS
19	Catalytic conversion of simple haloporphyrins into alkyl-, aryl-, pyridyl-, and vinyl-substituted porphyrins. Journal of the American Chemical Society, 1993, 115, 2513-2515.	13.7	148
20	Singlet and Triplet Excited States of Emissive, Conjugated Bis(porphyrin) Compounds Probed by Optical and EPR Spectroscopic Methods. Journal of the American Chemical Society, 2000, 122, 7017-7033.	13.7	145
21	EPR Spectroscopy and Photophysics of the Lowest Photoactivated Triplet State of a Series of Highly Conjugated (Porphinato)Zn Arrays. Journal of the American Chemical Society, 1995, 117, 12514-12527.	13.7	136
22	Decoupling Optical and Potentiometric Band Gaps in π-Conjugated Materials. Journal of the American Chemical Society, 2002, 124, 8550-8552.	13.7	133
23	Electronic Stark Effect Studies of a Porphyrin-Based Pushâ^Pull Chromophore Displaying a Large First Hyperpolarizability:  State-Specific Contributions to β. Journal of the American Chemical Society, 1998, 120, 2606-2611.	13.7	131
24	Plasmon-Induced Electrical Conduction in Molecular Devices. ACS Nano, 2010, 4, 1019-1025.	14.6	131
25	Supermolecular-Chromophore-Sensitized Near-Infrared-to-Visible Photon Upconversion. Journal of the American Chemical Society, 2010, 132, 14203-14211.	13.7	131
26	Tat-Functionalized Near-Infrared Emissive Polymersomes for Dendritic Cell Labeling. Bioconjugate Chemistry, 2007, 18, 31-40.	3.6	128
27	Ultrafast Singlet Excited-State Polarization in Electronically Asymmetric Ethyne-Bridged Bis[(porphinato)zinc(II)] Complexes. Journal of the American Chemical Society, 2003, 125, 2687-2696.	13.7	124
28	Conjugated Chromophore Arrays with Unusually Large Hole Polaron Delocalization Lengths. Journal of the American Chemical Society, 2006, 128, 8380-8381.	13.7	121
29	Potentiometric, Electronic Structural, and Ground- and Excited-State Optical Properties of Conjugated Bis[(Porphinato)zinc(II)] Compounds Featuring Proquinoidal Spacer Units. Journal of the American Chemical Society, 2005, 127, 5186-5195.	13.7	114
30	Long-range electron transfer in ruthenium-modified cytochrome c: evaluation of porphyrin-ruthenium electronic couplings in the Candida krusei and horse heart proteins. Journal of the American Chemical Society, 1990, 112, 2420-2422.	13.7	113
31	De Novo Design and Molecular Assembly of a Transmembrane Diporphyrin-Binding Protein Complex. Journal of the American Chemical Society, 2010, 132, 15516-15518.	13.7	110
32	Facile Synthesis of meso-Tetrakis(perfluoroalkyl)porphyrins: Spectroscopic Properties and X-ray Crystal Structure of Highly Electron-Deficient 5,10,15,20-Tetrakis(heptafluoropropyl)porphyrin. Journal of Organic Chemistry, 1994, 59, 6943-6948.	3.2	103
33	Synthesis, Electronic Structure, and Electron Transfer Dynamics of (Aryl)ethynyl-Bridged Donorâ~'Acceptor Systems. Journal of the American Chemical Society, 2003, 125, 8769-8778.	13.7	102
34	Optimizing Single-Molecule Conductivity of Conjugated Organic Oligomers with Carbodithioate Linkers. Journal of the American Chemical Society, 2010, 132, 7946-7956.	13.7	102
35	Molecular Design of Porphyrin-Based Nonlinear Optical Materials. Journal of Physical Chemistry A, 2008, 112, 12203-12207.	2.5	100
36	De novo design of a hyperstable non-natural protein–ligand complex with sub-à accuracy. Nature Chemistry, 2017, 9, 1157-1164.	13.6	93

#	Article	IF	CITATIONS
37	Synthesis, Structure, Electronic Spectroscopy, Photophysics, Electrochemistry, and X-ray Photoelectron Spectroscopy of Highly-Electron-Deficient [5,10,15,20-Tetrakis(perfluoroalkyl)porphinato]zinc(II) Complexes and Their Free Base Derivatives. Journal of the American Chemical Society, 1996, 118, 8344-8354.	13.7	92
38	<i>In vivo</i> fluorescence imaging: a personal perspective. Wiley Interdisciplinary Reviews: Nanomedicine and Nanobiotechnology, 2009, 1, 156-167.	6.1	91
39	Effect of Solvent Polarity and Electrophilicity on Quantum Yields and Solvatochromic Shifts of Single-Walled Carbon Nanotube Photoluminescence. Journal of the American Chemical Society, 2012, 134, 12485-12491.	13.7	91
40	De Novo Design of a Single-Chain Diphenylporphyrin Metalloprotein. Journal of the American Chemical Society, 2007, 129, 10732-10740.	13.7	90
41	Quasi-Ohmic Single Molecule Charge Transport through Highly Conjugated <i>meso</i> -to- <i>meso</i> Ethyne-Bridged Porphyrin Wires. Nano Letters, 2012, 12, 2722-2727.	9.1	90
42	Leuko-polymersomes. Faraday Discussions, 2008, 139, 129.	3.2	85
43	Tunable Leuko-polymersomes That Adhere Specifically to Inflammatory Markers. Langmuir, 2010, 26, 14089-14096.	3.5	81
44	Syntheses, NMR and EPR Spectroscopy, Electrochemical Properties, and Structural Studies of [5,10,15,20-Tetrakis(perfluoroalkyl)porphinato]iron(II) and -iron(III) Complexes. Journal of the American Chemical Society, 1999, 121, 5196-5209.	13.7	74
45	Broad Spectral Domain Fluorescence Wavelength Modulation of Visible and Near-Infrared Emissive Polymersomes. Journal of the American Chemical Society, 2005, 127, 15388-15390.	13.7	73
46	Syntheses and1H NMR Spectroscopy of Rigid, Cofacially Aligned, Porphyrinâ^'Bridgeâ^'Quinone Systems in Which the Interplanar Separations between the Porphyrin, Aromatic Bridge, and Quinone Are Less than the Sum of Their Respective van der Waals Radii. Journal of the American Chemical Society, 2000, 122, 8717-8727.	13.7	71
47	Extreme Electronic Modulation of the Cofacial Porphyrin Structural Motif. Journal of the American Chemical Society, 2002, 124, 4298-4311.	13.7	70
48	Highly Conjugated (Polypyridyl)metalâ^'(Porphinato)zinc(II) Compounds:Â Long-Lived, High Oscillator Strength, Excited-State Absorbers Having Exceptional Spectral Coverage of the Near-Infrared. Journal of the American Chemical Society, 2004, 126, 9474-9475.	13.7	69
49	Photoinitiated Destruction of Composite Porphyrinâ^'Protein Polymersomes. Journal of the American Chemical Society, 2009, 131, 3872-3874.	13.7	69
50	Two-Photon Absorption Properties of Proquinoidal D-A-D and A-D-A Quadrupolar Chromophores. Journal of Physical Chemistry A, 2011, 115, 5525-5539.	2.5	69
51	Single-Handed Helical Wrapping of Single-Walled Carbon Nanotubes by Chiral, Ionic, Semiconducting Polymers. Journal of the American Chemical Society, 2013, 135, 16220-16234.	13.7	68
52	Porphyrin-Quinone Electron Transfer Revisited. The Role of Excited-State Degeneracy in Ultrafast Charge Transfer Reactions. Journal of the American Chemical Society, 1995, 117, 3749-3753.	13.7	67
53	Quantitative membrane loading of polymer vesicles. Soft Matter, 2006, 2, 973.	2.7	67
54	Distance Dependence of Electron Transfer in Rigid, Cofacially Compressed, ï€-Stacked Porphyrinâ^'Bridgeâ^'Quinone Systems. Journal of the American Chemical Society, 2002, 124, 8275-8279.	13.7	66

#	Article	IF	CITATIONS
55	Dynamics and Transient Absorption Spectral Signatures of the Single-Wall Carbon Nanotube Electronically Excited Triplet State. Journal of the American Chemical Society, 2011, 133, 17156-17159.	13.7	66
56	Strongly Coupled Porphyrin Arrays Featuring Both π-Cofacial and Linear-π-Conjugative Interactions. Inorganic Chemistry, 2002, 41, 331-341.	4.0	65
57	Using α-Helical Coiled-Coils to Design Nanostructured Metalloporphyrin Arrays. Journal of the American Chemical Society, 2008, 130, 11921-11927.	13.7	63
58	Aqueous self-assembly of poly(ethylene oxide)-block-poly(Îμ-caprolactone) (PEO-b-PCL) copolymers: disparate diblock copolymer compositions give rise to nano- and meso-scale bilayered vesicles. Nanoscale, 2013, 5, 10908.	5.6	63
59	Printable and recyclable carbon electronics using crystalline nanocellulose dielectrics. Nature Electronics, 2021, 4, 261-268.	26.0	62
60	Synthesis, Transient Absorption, and Transient Resonance Raman Spectroscopy of Novel Electron Donorâ^'Acceptor Complexes:  [5,15-Bis[(4â€~-nitrophenyl)ethynyl]-10,20- diphenylporphinato]copper(II) anc [5-[[4â€~-(Dimethylamino)phenyl]ethynyl]-15-[(4â€~ã€~-nitrophenyl)ethynyl]-10,20-diphenylporphinato]copper(II) Journal of the American Chemical Society, 1997, 119, 12578-12589.). ^{13.7}	61
61	Transition-Metal-Mediated [2 + 2 + 2] Cycloaddition Reactions with Ethyne-Containing Porphyrin Templates:Â New Routes to Cofacial Porphyrin Structures and Facially-Functionalized (Porphinato)metal Species. Journal of the American Chemical Society, 2000, 122, 12393-12394.	13.7	60
62	Molecular Symmetry and Solutionâ€Phase Structure Interrogated by Hyperâ€Rayleigh Depolarization Measurements: Elaborating Highly Hyperpolarizable <i>D</i> ₂ ‣ymmetric Chromophores. Angewandte Chemie - International Edition, 2008, 47, 2978-2981.	13.8	59
63	Kinetics of disproportionation of tricarbonylbis(phosphine)iron(I) cation radicals probed by double potential step chronocoulometry. Journal of the American Chemical Society, 1986, 108, 4037-4042.	13.7	57
64	Generalized Mullikenâ^'Hush Analysis of Electronic Coupling Interactions in Compressed Ï€-Stacked Porphyrinâ^'Bridgeâ^'Quinone Systems. Journal of the American Chemical Society, 2005, 127, 11303-11310.	13.7	57
65	Molecular Engineering of Intensely Near-Infrared Absorbing Excited States in Highly Conjugated Oligo(porphinato)zincâ`'(Polypyridyl)metal(II) Supermolecules. Journal of the American Chemical Society, 2007, 129, 9691-9703.	13.7	57
66	Carrier Dynamics Engineering for High-Performance Electron-Transport-Layer-free Perovskite Photovoltaics. CheM, 2018, 4, 2405-2417.	11.7	57
67	Predicting the Frequency Dispersion of Electronic Hyperpolarizabilities on the Basis of Absorption Data and Thomasâ~'Kuhn Sum Rules. Journal of Physical Chemistry C, 2010, 114, 2349-2359.	3.1	56
68	Sensing membrane stress with near IR-emissive porphyrins. Proceedings of the National Academy of Sciences of the United States of America, 2011, 108, 13984-13989.	7.1	56
69	Computational de Novo Design and Characterization of a Protein That Selectively Binds a Highly Hyperpolarizable Abiological Chromophore. Journal of the American Chemical Society, 2013, 135, 13914-13926.	13.7	55
70	Exploiting Plasmon-Induced Hot Electrons in Molecular Electronic Devices. ACS Nano, 2013, 7, 4479-4486.	14.6	55
71	Tailoring Porphyrin-Based Electron Accepting Materials for Organic Photovoltaics. Journal of the American Chemical Society, 2014, 136, 17561-17569.	13.7	55
72	Computational Design and Elaboration of a de Novo Heterotetrameric α-Helical Protein That Selectively Binds an Emissive Abiological (Porphinato)zinc Chromophore. Journal of the American Chemical Society, 2010, 132, 3997-4005.	13.7	54

#	Article	IF	CITATIONS
73	The Roles of Molecular Structure and Effective Optical Symmetry in Evolving Dipolar Chromophoric Building Blocks to Potent Octopolar Nonlinear Optical Chromophores. Journal of the American Chemical Society, 2011, 133, 2884-2896.	13.7	54
74	Mean Firstâ€Passage Times in Biology. Israel Journal of Chemistry, 2016, 56, 816-824.	2.3	54
75	Mechanistic Studies of (Porphinato)Iron-Catalyzed Isobutane Oxidation. Comparative Studies of Three Classes of Electron-Deficient Porphyrin Catalysts. Inorganic Chemistry, 2000, 39, 3125-3139.	4.0	53
76	The Effect of Molecular Orientation on the Potential of Porphyrinâ^'Metal Contacts. Nano Letters, 2008, 8, 110-113.	9.1	53
77	Mechanism of oxidatively induced migratory insertion of carbon monoxide. Evidence for a nineteen-electron intermediate. Journal of the American Chemical Society, 1987, 109, 5127-5133.	13.7	51
78	Composite Electronic Materials Based on Poly(3,4-propylenedioxythiophene) and Highly Charged Poly(aryleneethynylene)-Wrapped Carbon Nanotubes for Supercapacitors. ACS Applied Materials & Interfaces, 2012, 4, 102-109.	8.0	51
79	Synthesis of amines through nucleophilic addition on nitrogen. Journal of the American Chemical Society, 1984, 106, 5753-5754.	13.7	48
80	Controlling Bulk Optical Properties of Emissive Polymersomes through Intramembranous Polymerâ^Fluorophore Interactions. Chemistry of Materials, 2007, 19, 1309-1318.	6.7	48
81	Single‣tep Assembly of Multimodal Imaging Nanocarriers: MRI and Longâ€Wavelength Fluorescence Imaging. Advanced Healthcare Materials, 2015, 4, 1376-1385.	7.6	48
82	Extreme electron polaron spatial delocalization in π-conjugated materials. Proceedings of the National Academy of Sciences of the United States of America, 2015, 112, 13779-13783.	7.1	48
83	Large Hyperpolarizabilities at Telecommunication-Relevant Wavelengths in Donor–Acceptor–Donor Nonlinear Optical Chromophores. ACS Central Science, 2016, 2, 954-966.	11.3	48
84	Impact of Electronic Asymmetry on Photoexcited Triplet-State Spin Distributions in Conjugated Porphyrin Oligomers Probed via EPR Spectroscopy. Journal of Physical Chemistry B, 2004, 108, 11893-11903.	2.6	47
85	Electronic Transport in Porphyrin Supermolecule-Gold Nanoparticle Assemblies. Nano Letters, 2012, 12, 2414-2419.	9.1	46
86	Ultrafast Excited-State Dynamics of Nanoscale Near-Infrared Emissive Polymersomes. Journal of the American Chemical Society, 2008, 130, 9773-9784.	13.7	45
87	Excitation of Highly Conjugated (Porphinato)palladium(II) and (Porphinato)platinum(II) Oligomers Produces Long-Lived, Triplet States at Unit Quantum Yield That Absorb Strongly over Broad Spectral Domains of the NIR. Journal of Physical Chemistry B, 2010, 114, 14696-14702.	2.6	44
88	In Vivo Dendritic Cell Tracking Using Fluorescence Lifetime Imaging and Near-Infrared-Emissive Polymersomes. Molecular Imaging and Biology, 2009, 11, 167-177.	2.6	43
89	Electron transfer reactions of rigid, cofacially compressed, ï€-stacked porphyrin–bridge–quinone systems. Coordination Chemistry Reviews, 2011, 255, 804-824.	18.8	43
90	Interrogating Conformationally Dependent Electron-Transfer Dynamics via Ultrafast Visible Pump/IR Probe Spectroscopy. Journal of the American Chemical Society, 2004, 126, 2684-2685.	13.7	42

#	Article	IF	CITATIONS
91	Near-Infrared Optical Imaging of B16 Melanoma Cells via Low-Density Lipoprotein-Mediated Uptake and Delivery of High Emission Dipole Strength Tris[(porphinato)zinc(II)] Fluorophores. Bioconjugate Chemistry, 2005, 16, 542-550.	3.6	42
92	Amphiphilic Four-Helix Bundle Peptides Designed for Light-Induced Electron Transfer Across a Soft Interface. Nano Letters, 2005, 5, 1658-1667.	9.1	41
93	Solvent- and Wavelength-Dependent Photoluminescence Relaxation Dynamics of Carbon Nanotube sp ³ Defect States. ACS Nano, 2018, 12, 8060-8070.	14.6	41
94	One- and two-photon absorption of highly conjugated multiporphyrin systems in the two-photon Soret transition region. Journal of Chemical Physics, 2009, 130, 134506.	3.0	40
95	Phase Transfer Catalysts Drive Diverse Organic Solvent Solubility of Single-Walled Carbon Nanotubes Helically Wrapped by Ionic, Semiconducting Polymers. Nano Letters, 2010, 10, 4192-4199.	9.1	40
96	Ethyne-Bridged (Porphinato)Zinc(II)â^'(Porphinato)Iron(III) Complexes:Â Phenomenological Dependence of Excited-State Dynamics upon (Porphinato)Iron Electronic Structure. Journal of the American Chemical Society, 2006, 128, 10423-10435.	13.7	39
97	A Generalized System for Photoresponsive Membrane Rupture in Polymersomes. Advanced Functional Materials, 2010, 20, 2588-2596.	14.9	39
98	Incorporation of Designed Extended Chromophores into Amphiphilic 4-Helix Bundle Peptides for Nonlinear Optical Biomolecular Materials. Nano Letters, 2006, 6, 2387-2394.	9.1	38
99	How to improve your image. Nature, 2009, 458, 716-717.	27.8	38
100	Structural and pH Dependence of Excited State PCET Reactions Involving Reductive Quenching of the MLCT Excited State of [Ru ^{II} (bpy) ₂ (bpz)] ²⁺ by Hydroquinones. Journal of Physical Chemistry A, 2011, 115, 3346-3356.	2.5	37
101	On the Importance of Electronic Symmetry for Triplet State Delocalization. Journal of the American Chemical Society, 2017, 139, 5301-5304.	13.7	37
102	The Degree of Charge Transfer in Ground and Charge-Separated States Revealed by Ultrafast Visible Pump/Mid-IR Probe Spectroscopy. Journal of the American Chemical Society, 2004, 126, 5022-5023.	13.7	36
103	Electronic Modulation of Hyperpolarizable (Porphinato)zinc(II) Chromophores Featuring Ethynylphenyl-, Ethynylthiophenyl-, Ethynylthiazolyl-, and Ethynylbenzothiazolyl-Based Electron-Donating and -Accepting Moieties. Inorganic Chemistry, 2006, 45, 9703-9712.	4.0	36
104	Origins of the Helical Wrapping of Phenyleneethynylene Polymers about Single-Walled Carbon Nanotubes. Journal of Physical Chemistry B, 2013, 117, 12953-12965.	2.6	35
105	Mapping hole hopping escape routes in proteins. Proceedings of the National Academy of Sciences of the United States of America, 2019, 116, 15811-15816.	7.1	35
106	Allosteric cooperation in a de novo-designed two-domain protein. Proceedings of the National Academy of Sciences of the United States of America, 2020, 117, 33246-33253.	7.1	35
107	Valence Band Dependent Charge Transport in Bulk Molecular Electronic Devices Incorporating Highly Conjugated Multi-[(Porphinato)Metal] Oligomers. Journal of the American Chemical Society, 2016, 138, 2078-2081.	13.7	34
108	Synthesis, Excited-State Dynamics, and Reactivity of a Directly-Linked Pyromellitimideâ^'(Porphinato)zinc(II) Complex. Inorganic Chemistry, 2002, 41, 566-570.	4.0	33

#	Article	IF	CITATIONS
109	Synthesis of Water-Soluble Poly(<i>p</i> -phenyleneethynylene) in Neat Water under Aerobic Conditions via Suzuki-Miyaura Polycondensation Using a Diborylethyne Synthon. Organic Letters, 2008, 10, 1341-1344.	4.6	33
110	Design of Coupled Porphyrin Chromophores with Unusually Large Hyperpolarizabilities. Journal of Physical Chemistry C, 2012, 116, 9724-9733.	3.1	33
111	Near-Infrared-to-Visible Photon Upconversion Enabled by Conjugated Porphyrinic Sensitizers under Low-Power Noncoherent Illumination. Journal of Physical Chemistry A, 2015, 119, 5642-5649.	2.5	33
112	Alkyne-Bridged Multi[Copper(II) Porphyrin] Structures: Nuances of Orbital Symmetry in Long-Range, Through-Bond Mediated, Isotropic Spin Exchange Interactions. Journal of the American Chemical Society, 2017, 139, 9759-9762.	13.7	33
113	Low-Resistance Molecular Wires Propagate Spin-Polarized Currents. Journal of the American Chemical Society, 2019, 141, 14707-14711.	13.7	33
114	Tricarbonylbis(phosphine)iron(I) cation radicals. A spectroscopic and theoretical study. Journal of the American Chemical Society, 1986, 108, 3697-3702.	13.7	31
115	High-Pressure NMR Studies of (Porphinato)iron-Catalyzed Isobutane Oxidation Utilizing Dioxygen as the Stoichiometric Oxidant. Journal of the American Chemical Society, 1997, 119, 1791-1792.	13.7	31
116	Trends in triplet excitation delocalization in highly conjugated (porphinato)zinc(II) arrays probed by EPR spectroscopy. Synthetic Metals, 2001, 116, 247-253.	3.9	31
117	Defusing redox bombs?. Proceedings of the National Academy of Sciences of the United States of America, 2015, 112, 10821-10822.	7.1	30
118	Molecular Road Map to Tuning Ground State Absorption and Excited State Dynamics of Long-Wavelength Absorbers. Journal of the American Chemical Society, 2017, 139, 16946-16958.	13.7	30
119	Structural Studies of Amphiphilic 4-Helix Bundle Peptides Incorporating Designed Extended Chromophores for Nonlinear Optical Biomolecular Materials. Nano Letters, 2006, 6, 2395-2405.	9.1	29
120	Hapticity-Dependent Charge Transport through Carbodithioate-Terminated [5,15-Bis(phenylethynyl)porphinato]zinc(II) Complexes in Metal–Molecule–Metal Junctions. Nano Letters, 2014, 14, 5493-5499.	9.1	29
121	Fluence-Dependent Singlet Exciton Dynamics in Length-Sorted Chirality-Enriched Single-Walled Carbon Nanotubes. Nano Letters, 2014, 14, 504-511.	9.1	27
122	Electrochemical studies of an oxidatively induced ring slippage in 17-electron (η3-indenyl)(η5-indenyl)V(CO)2. Journal of Organometallic Chemistry, 1990, 383, 271-278.	1.8	26
123	Temperature-Dependent Mechanistic Transition for Photoinduced Electron Transfer Modulated by Excited-State Vibrational Relaxation Dynamicsâ€. Journal of Physical Chemistry B, 2007, 111, 6829-6838.	2.6	26
124	Theoretical study of bimolecular nucleophilic substitution at four, five-, and six-coordinate metal carbonyl radicals. Journal of the American Chemical Society, 1988, 110, 4942-4953.	13.7	25
125	Dynamics of charged excitons in electronically and morphologically homogeneous single-walled carbon nanotubes. Proceedings of the National Academy of Sciences of the United States of America, 2018, 115, 674-679.	7.1	25
126	Europium- and lithium-doped yttrium oxide nanocrystals that provide a linear emissive response with X-ray radiation exposure. Nanoscale, 2014, 6, 5284-5288.	5.6	23

#	Article	IF	CITATIONS
127	Potentiometric, Electronic, and Transient Absorptive Spectroscopic Properties of Oxidized Single-Walled Carbon Nanotubes Helically Wrapped by Ionic, Semiconducting Polymers in Aqueous and Organic Media. Journal of the American Chemical Society, 2014, 136, 14193-14199.	13.7	23
128	Electronic and optical properties of Er-doped Y ₂ O ₂ S phosphors. Journal of Materials Chemistry C, 2015, 3, 11486-11496.	5.5	23
129	Electronic structure and photophysics of a supermolecular iron complex having a long MLCT-state lifetime and panchromatic absorption. Proceedings of the National Academy of Sciences of the United States of America, 2020, 117, 20430-20437.	7.1	23
130	Control of the Orientational Order and Nonlinear Optical Response of the "Push-Pull―Chromophore RuPZn via Specific Incorporation into Densely Packed Monolayer Ensembles of an Amphiphilic Four-Helix Bundle Peptide: Characterization of the Peptideâ^Chromophore Complexes. Journal of the American Chemical Society, 2010, 132, 11083-11092.	13.7	22
131	Photoinduced Electron Transfer Elicits a Change in the Static Dielectric Constant of a <i>de Novo</i> Designed Protein. Journal of the American Chemical Society, 2016, 138, 2130-2133.	13.7	22
132	Carbodithioate-Terminated Oligo(phenyleneethynylene)s:Â Synthesis and Surface Functionalization of Gold Nanoparticles. Organic Letters, 2007, 9, 2779-2782.	4.6	20
133	<i>>De Novo</i> Design, Solution Characterization, and Crystallographic Structure of an Abiological Mn–Porphyrin-Binding Protein Capable of Stabilizing a Mn(V) Species. Journal of the American Chemical Society, 2021, 143, 252-259.	13.7	19
134	Control of the Orientational Order and Nonlinear Optical Response of the "Pushâ 'Pull― Chromophore RuPZn via Specific Incorporation into Densely Packed Monolayer Ensembles of an Amphiphilic 4-Helix Bundle Peptide: Second Harmonic Generation at High Chromophore Densities. Journal of the American Chemical Society, 2010, 132, 9693-9700.	13.7	18
135	Soft biodegradable polymersomes from caprolactone-derived polymers. Soft Matter, 2012, 8, 10853.	2.7	18
136	Electron Spin Relaxation of Hole and Electron Polarons in π-Conjugated Porphyrin Arrays: Spintronic Implications. Journal of Physical Chemistry B, 2015, 119, 7681-7689.	2.6	18
137	Fiberâ€optic detector for real time dosimetry of a microâ€planar xâ€ray beam. Medical Physics, 2015, 42, 1966-1972.	3.0	18
138	Real-time dose-rate monitoring with gynecologic brachytherapy: Results of an initial clinical trial. Brachytherapy, 2018, 17, 1023-1029.	0.5	18
139	Modulation of Dark Conductivity over a 1 × 10â^'12 to 1 × 10â^'5 S/cm Range Through Ancillary Group Modification in Amorphous Solids of Ethyne-Bridged (Porphinato)zinc(II) Oligomers. Chemistry of Materials, 2007, 19, 6062-6064.	6.7	17
140	One-Pot Solvothermal Synthesis of Highly Emissive, Sodium-Codoped, LaF3 and BaLaF5 Core-Shell Upconverting Nanocrystals. Nanomaterials, 2014, 4, 69-86.	4.1	17
141	Unambiguous Diagnosis of Photoinduced Charge Carrier Signatures in a Stoichiometrically Controlled Semiconducting Polymerâ€Wrapped Carbon Nanotube Assembly. Angewandte Chemie - International Edition, 2015, 54, 8133-8138.	13.8	17
142	NIR-emissive PEG-b-TCL micelles for breast tumor imaging and minimally invasive pharmacokinetic analysis. Nanoscale, 2017, 9, 13465-13476.	5.6	17
143	Synthetic Control of Exciton Dynamics in Bioinspired Cofacial Porphyrin Dimers. Journal of the American Chemical Society, 2022, 144, 6298-6310.	13.7	17
144	Synthesis of (porphinato)zinc(II)-spacer-(porphinato)iron(III) chloride complexes: a modular approach to fixed-distance electron-transfer model compounds through the efficacy of metal-mediated cross-coupling. Inorganica Chimica Acta, 1996, 242, 211-218.	2.4	16

#	Article	IF	CITATIONS
145	High-Resolution Structure and Conformational Dynamics of Rigid, Cofacially Aligned Porphyrinâ^'Bridgeâ^'Quinone Systems As Determined by NMR Spectroscopy and ab Initio Simulated Annealing Calculations. Journal of the American Chemical Society, 2001, 123, 5668-5679.	13.7	16
146	Near IR nonlinear absorption of an organic supermolecule [Invited]. Optical Materials Express, 2011, 1, 1383.	3.0	16
147	Controlling Polarization Dependent Reactions to Fabricate Multiâ€Component Functional Nanostructures. Advanced Functional Materials, 2011, 21, 4712-4718.	14.9	16
148	The evolution of spin distribution in the photoexcited triplet state of ethyne-elaborated porphyrins. Chemical Communications, 2013, 49, 9722.	4.1	16
149	Ionic Selfâ€Assembly Provides Dense Arrays of Individualized, Aligned Singleâ€Walled Carbon Nanotubes. Angewandte Chemie - International Edition, 2013, 52, 13080-13085.	13.8	16
150	Controlling the excited-state dynamics of low band gap, near-infrared absorbers via proquinoidal unit electronic structural modulation. Chemical Science, 2017, 8, 5889-5901.	7.4	16
151	Raman Spectroscopic Investigation of Individual Single-Walled Carbon Nanotubes Helically Wrapped by Ionic, Semiconducting Polymers. Journal of Physical Chemistry C, 2013, 117, 14840-14849.	3.1	15
152	Selective loss of CO in the photochemistry of MnRe(CO)10: a study using matrix isolation and time-resolved infrared spectroscopy. Journal of Organometallic Chemistry, 1987, 331, 347-355.	1.8	14
153	Power-Dependent Radiant Flux and Absolute Quantum Yields of Upconversion Nanocrystals under Continuous and Pulsed Excitation. Journal of Physical Chemistry C, 2018, 122, 252-259.	3.1	14
154	Structure and Dynamics of an Extended Conjugated NLO Chromophore within an Amphiphilic 4-Helix Bundle Peptide by Molecular Dynamics Simulation. Journal of Physical Chemistry B, 2008, 112, 1350-1357.	2.6	13
155	EPR of Photoexcited Triplet-State Acceptor Porphyrins. Journal of Physical Chemistry C, 2021, 125, 11782-11790.	3.1	13
156	Probing polarization and dielectric function of molecules with higher order harmonics in scattering–near-field scanning optical microscopy. Journal of Applied Physics, 2009, 106, 114307.	2.5	12
157	Caging Metal Ions with Visible Light-Responsive Nanopolymersomes. Langmuir, 2015, 31, 799-807.	3.5	12
158	Design of diethynyl porphyrin derivatives with high near infrared fluorescence quantum yields. Journal of Porphyrins and Phthalocyanines, 2015, 19, 205-218.	0.8	12
159	Driving high quantum yield NIR emission through proquinoidal linkage motifs in conjugated supermolecular arrays. Chemical Science, 2020, 11, 8095-8104.	7.4	11
160	Engineering High-Potential Photo-oxidants with Panchromatic Absorption. Journal of the American Chemical Society, 2017, 139, 8412-8415.	13.7	10
161	Synthesis and characterization of Na(Gd0.5Lu0.5)F4: Nd3+,a core-shell free multifunctional contrast agent. Journal of Alloys and Compounds, 2017, 695, 280-285.	5.5	10
162	Excitation energy-dependent photocurrent switching in a single-molecule photodiode. Proceedings of the United States of America, 2019, 116, 16198-16203.	7.1	10

#	Article	IF	CITATIONS
163	Engineering opposite electronic polarization of singlet and triplet states increases the yield of high-energy photoproducts. Proceedings of the National Academy of Sciences of the United States of America, 2019, 116, 14465-14470.	7.1	10
164	Distance Dependence of Electronic Coupling in Rigid, Cofacially Compressed, ï€-Stacked Organic Mixed-Valence Systems. Journal of Physical Chemistry B, 2020, 124, 1033-1048.	2.6	9
165	Unambiguous Diagnosis of Photoinduced Charge Carrier Signatures in a Stoichiometrically Controlled Semiconducting Polymerâ€Wrapped Carbon Nanotube Assembly. Angewandte Chemie, 2015, 127, 8251-8256.	2.0	8
166	Orientational Dependence of Cofacial Porphyrin–Quinone Electronic Interactions within the Strong Coupling Regime. Journal of Physical Chemistry B, 2019, 123, 10456-10462.	2.6	8
167	Twisted molecular wires polarize spin currents at room temperature. Proceedings of the National Academy of Sciences of the United States of America, 2022, 119, .	7.1	8
168	Acentric 2-D Ensembles of D-br-A Electron-Transfer Chromophores via Vectorial Orientation within Amphiphilic <i>n</i> -Helix Bundle Peptides for Photovoltaic Device Applications. Langmuir, 2012, 28, 3227-3238.	3.5	7
169	First-order hyperpolarizabilities of chiral, polymer-wrapped single-walled carbon nanotubes. Chemical Communications, 2016, 52, 12206-12209.	4.1	6
170	Coordination Compounds for Functional Nonlinear Optics: Enhancing and Switching the Second-Order Nonlinear Optical Responses. ACS Symposium Series, 2006, , 527-540.	0.5	5
171	Quantitative Evaluation of Optical Free Carrier Generation in Semiconducting Single-Walled Carbon Nanotubes. Journal of the American Chemical Society, 2018, 140, 14619-14626.	13.7	5
172	Topology, Distance, and Orbital Symmetry Effects on Electronic Spin–Spin Couplings in Rigid Molecular Systems: Implications for Long-Distance Spin–Spin Interactions. Journal of Physical Chemistry A, 2020, 124, 7411-7415.	2.5	5
173	Femtosecond pulse train shaping improves two-photon excited fluorescence measurements. Optics Letters, 2014, 39, 5606.	3.3	4
174	Spinning Molecules, Spinning Spins: Modulation of an Electron Spin Exchange Interaction in a Highly Anisotropic Hyperfine Field. ACS Omega, 2021, 6, 27865-27873.	3.5	4
175	Enhanced dispersion of CdSe/MEH-CN-PPV hybrid nanocomposites by in situ polymerization using AEM as photopolymerizable precursor. Colloid and Polymer Science, 2012, 290, 1501-1509.	2.1	3
176	Biodegradable Polymersomes for the Delivery of Gemcitabine to Panc-1 Cells. Journal of Pharmaceutics, 2013, 2013, 1-10.	4.7	3
177	A High Precision In-Vivo Dosimeter for Real Time Quality Assurance in HDR Brachytherapy, Based Off a Nano-crystalline Scintillator Fiber-Optic Radiation Sensor. Brachytherapy, 2015, 14, S27-S28.	0.5	3
178	Excited-State Dynamics and Nonlinear Optical Properties of Hyperpolarizable Chromophores Based on Conjugated Bis(terpyridyl)Ru(II) and Palladium and Platinum Porphyrinic Components: Impact of Heavy Metals upon Supermolecular Electro-Optic Properties. Inorganic Chemistry, 2021, 60, 15404-15412.	4.0	2
179	Composite Electronic Materials for Supercapacitor Applications. ECS Transactions, 2009, 23, 3-10.	0.5	1
180	Optoelectronic Devices: Controlling Polarization Dependent Reactions to Fabricate Multi-Component Functional Nanostructures (Adv. Funct. Mater. 24/2011). Advanced Functional Materials, 2011, 21, 4598-4598.	14.9	1

#	Article	IF	CITATIONS
181	Unusual solvent polarity dependent excitation relaxation dynamics of a bis[<i>p</i> -ethynyldithiobenzoato]Pd-linked bis[(porphinato)zinc] complex. Molecular Systems Design and Engineering, 2018, 3, 275-284.	3.4	1
182	Tribute to David N. Beratan. Journal of Physical Chemistry B, 2020, 124, 3437-3440.	2.6	0